

# Optical Engineering

OpticalEngineering.SPIEDigitalLibrary.org

## Single-exposure multiphoton fabrication of polygonized structures by an SLM-modulated Fresnel zone lens

Chenchu Zhang  
Yanlei Hu  
Jiawen Li  
Zhaoxin Lao  
Bing Xu  
Jincheng Ni  
Ze Cai  
Dong Wu  
Jiaru Chu

**SPIE.**

Chenchu Zhang, Yanlei Hu, Jiawen Li, Zhaoxin Lao, Bing Xu, Jincheng Ni, Ze Cai, Dong Wu, Jiaru Chu, "Single-exposure multiphoton fabrication of polygonized structures by an SLM-modulated Fresnel zone lens," *Opt. Eng.* **55**(3), 035102 (2016), doi: 10.1117/1.OE.55.3.035102.

# Single-exposure multiphoton fabrication of polygonized structures by an SLM-modulated Fresnel zone lens

Chenchu Zhang, Yanlei Hu,\* Jiawen Li, Zhaoxin Lao, Bing Xu, Jincheng Ni, Ze Cai, Dong Wu, and Jiaru Chu

University of Science and Technology of China, Department of Precision Machinery and Precision Instrumentation, Room 303, Third Mechanical Building, No. 443, Huangshan Road, Hefei, China

**Abstract.** Recently, annular beams have been developed to rapidly fabricate microscope tubular structures via two-photon polymerization, but the distribution of the light field is limited to a ring pattern. Here a Fresnel lens is designed and applied to modulate the light field into a uniform quadrangle or hexagon shape with controllable diameters. By applying a spatial light modulator to load the phase information of the Fresnel lens, quadrangle and hexagon structures are achieved through single exposure of a femtosecond laser. A  $3 \times 6$  array of structures is made within 9 s. Comparing with the conventional holographic processing, this method shows higher uniformity, high efficiency, better flexibility, and easy operation. The approach exhibited a promising prospect in rapidly fabricating structures such as tissue engineering scaffolds and variously shaped tubular arrays. © 2016 Society of Photo-Optical Instrumentation Engineers (SPIE) [DOI: 10.1117/1.OE.55.3.035102]

Keywords: femtosecond laser; two-photon polymerization; shaped beam; spatial light modulator.

Paper 151440P received Oct. 14, 2015; accepted for publication Feb. 17, 2016; published online Mar. 11, 2016.

## 1 Introduction

Femtosecond induced two-photon polymerization (TPP) has been recently grown as one of the most promising approaches for the fabrication of micro-optical components,<sup>1-3</sup> micro/nanomachines,<sup>4</sup> microfluidic systems,<sup>5</sup> and so on.<sup>6,7</sup> In conventional direct writing TPP using a Gaussian light beam, the resulting volume pixel (voxel) is usually an ellipsoid with the long axis in the beam propagation direction.<sup>8</sup> Due to the simple shape of the voxel, a complex three-dimensional (3-D) structure could be fabricated dot by dot by scanning the focus. However, it is time consuming in fabricating structures with large volumes. To overcome this bottle neck, a variety of methods such as introducing microlens arrays,<sup>9</sup> a spatial light modulator (SLM),<sup>10</sup> or a multiplexed Fresnel lens (FL)<sup>11</sup> to split incident light into several beams have been developed for high efficiency TPP. Among these methods, the most widely used is the SLM due to its high flexibility of parallel fabrication. The distributions of the foci array can be arbitrarily controlled by designing the computer generated hologram on SLM.<sup>12</sup> With this approach, a variety of optical,<sup>13</sup> mechanical,<sup>14</sup> and biological<sup>15</sup> microstructures have been rapidly fabricated. However, this method is only suitable for fabricating microstructure arrays with the same morphology by multifocus scanning.<sup>15</sup> Several effective approaches such as orbital angular momentum,<sup>16</sup> Bessel beam,<sup>17</sup> and annular Fresnel lens<sup>18</sup> have been applied to shape the focal spot into a ring shape. They have been used to achieve a hollow micropillar by a single exposure. Comparing with the conventional voxel-to-voxel scanning strategy, the focus-shaped approaches can produce ring-shaped 3-D structures with ultrahigh efficiency. These ring-shaped structures can be applied in many important practical fields such as biologic sensing,<sup>19</sup> cell controlling,<sup>20</sup> localized drug delivery,<sup>21</sup> catalysts,<sup>22</sup> and other microfluidic applications.<sup>23</sup> However, the existing focus-shaped approaches can only be applied in fabricating

ring-shaped structures. At the same time, annular structures are not able to produce a close packing array, which has a 100% fill factor. Hence, an approach which can rapidly fabricate polygonal structures, such as, quadrangles and hexagons, is necessary for both improving the flexibility of focus-shaped approaches and fabricating a close-packed array.

In this paper, a Fresnel zone lens is designed and applied to modulate the light field into a polygonal pattern. A single exposure approach based on this Fresnel zone lens is developed to rapidly fabricate micropolygonal arrays. Simulations and experimental verifications are made to prove the feasibility of this approach in fabricating nonclose-packed and close-packed polygonal arrays. Furthermore, we also proposed an efficient approach for producing a polygonal structure array within several seconds.

## 2 Generation and Simulation of Polygonal Fresnel Lens

### 2.1 Generation of Polygonal Fresnel Lens

As we know, the phase transformation of a spherical FL and that of a spherical lens follows the same transmission function, which is  $t = \exp[-ik(r^2)/2z]$ . Here,  $r$  is the distance to the center of lens.  $z$  is the distance from the lens back surface to the observation plane.  $k$  is the wavenumber. Thus, a spherical FL can focus light into a single dot, similar to the focusing ability of a spherical lens.

Hasegawa et al.<sup>11</sup> have shaped the focus into a dual point by multiplexing the FL. Here, we aim to design a new kind of FL which can shape the focus into a continuous polygon. In order to generate a polygonal-shaped focus instead of a single dot, we tried to move the FL following a polygonal path to generate a polygon-shaped focus instead of a single point. The polygonal Fresnel lens (PFL) can be described as a conventional FL shifting from the center with a distance  $n(\theta)r_0$ ,

\*Address all correspondence to: Yanlei Hu, E-mail: huyl@ustc.edu.cn

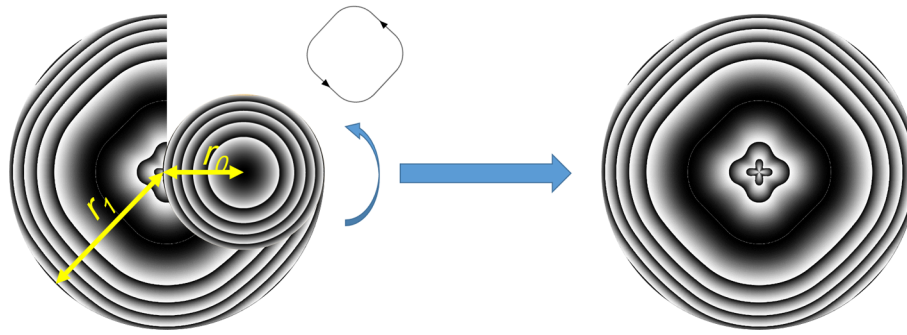


**Fig. 1** The image on the left is a diagrammatic sketch of the generation process of a PFL. The smaller circle is FL.  $r_0$  is the shift distance of FL, which is same as the radius of FL here.  $r_1$  is the radius of PFL. The FL rotates around the center of the FL, following a polygonal path. The image on the right is the finished PFL.

then moving around the center along a polygonal path.  $n(\theta)r_0$  corresponds to the shift distance and varies as a function of the azimuthal angle. This makes the zero-order plane of PFL a polygonal shape. As shown in Fig. 1,  $r_1$  is the radius of the PFL, and  $r_0$  is the distance from the center of the PFL to the center of the FL. If the shift distance is smaller than half of the radius of the PFL, that is,  $r_1 > 2 \times r_0$ , some parts of FL will overlap when rotating around the center, and the overlapped parts will be cut. Then the phase of PFL will be  $t = \exp\{-ik[r - n(\theta)r_0]^2/2z\}$ . Here  $n(\theta)r_0$  is the distance from the zero-order plane to the center of PFL. With these changes, the zero-order plane shifts from the center to the side of the PFL. The width of higher order planes follows the same rule as the FL.

## 2.2 Simulation Results

To further investigate the properties of PFL, we perform a numerical analysis to study its focusing ability with the help of the Huygens–Fresnel diffractive integral.<sup>24</sup> The propagation field at the observation plane can be deduced from the initial field at the backside of the PFL, according to the following expression:

$$E(x, y, z) = \frac{\exp(ikz)}{i\lambda z} \iint_{-\infty}^{\infty} E(x_1, y_1) \times \exp\left\{\frac{ik}{2z}[(x - x_1)^2 + (y - y_1)^2]\right\} dx_1 dy_1. \quad (1)$$

Here,  $x, y$  are the coordinates for the initial field at the backside of the lens.  $x_1, y_1$  are the coordinates at the observation plane.  $z$  is the distance from the lens back surface to the observation plane.  $k$  is the wavenumber. To better simulate the PFL displaying on an SLM, we pixelate the PFL with the pixel size of  $8 \mu\text{m} \times 8 \mu\text{m}$ , which is the same with the SLM used in the experiment.

Figure 2 is the simulation result of different PFLs with a zero-order width of 250 pixels. Figures 2(a)–2(c) are the distribution at the focal plane of different PFLs. The PFLs used to generate the focus are shown at the top-right corner. The shapes of focus are a quadrangle, hexagon, and octagon, with the uniformities of 87.0%, 85.3%, and 82.1%, respectively, showing that the PFLs can generate different focal distributions with high intensity uniformity. The uniformity is calculated by comparing the intensity peak of each azimuth angle. The formula used is as follows:

$$\text{Uniformity} = 1 - \frac{I_{\max} - I_{\min}}{I_{\max} + I_{\min}}. \quad (2)$$

Figure 2(d) is the distribution of the quadrangle Fresnel lens at the meridian plane containing the optical axis. The cross-section at the focal plane, shown in Fig. 2(e), has two sharp intensity peaks, which can enhance the energy density of focus and be very useful in fabricating high resolution microscopic structures. The  $x$ -axis shows the position of intensity. The  $y$ -axis is the normalized power.

## 3 Experiment Setup

The laser source is a mode-locked Ti:sapphire ultrafast oscillator (Coherent, Chamleon Vision-S) with a central wavelength at 800 nm, pulse duration of 75 fs, and repetition rate at 80 MHz. The average power is about 3 W, modulated by a power attenuator consisting of a half-wave plate and a Glan laserprism. After passing a beam expander, the beam slightly overfills the active area of the SLM to ensure modulation effect. The SLM (Holoeye, pluto NIR-2) has  $1920 \times 1080$  pixels, with each pitch of  $8 \mu\text{m}$ . The central  $1080 \times 1080$  pixels are used in this work. The Fresnel zone lens displayed on the SLM has 256 gray levels corresponding to phase modulation from 0 to  $2\pi$ . A high-pass filter is placed at focal plane of the PFL to block the “central light.” The remainder of the modulated beam is captured by a collimating lens and focused through a microscope objective (100 $\times$ , 0.9 NA) into the sample plane. The photoresist used in this work is SZ-2080, provided by IESL-FORTH, Greece (Fig. 3).

## 4 Results and Discussion

Figure 4 shows a  $3 \times 6$  microquadrangle array. Each structure is fabricated by a single exposure for 400 ms. Therefore, the whole array can be achieved in 7.2 s by controlling the irradiated region in the  $x$ - $y$  plane via translational stages. It will cost at least several minutes to fabricate by a voxel-to-voxel scanning strategy. Figures 4(a) and 4(b) are optical microscopy and scanning electron microscope (SEM) images of a quadrangle array, showing the high uniformity in morphology of each structure. The length of a side is  $26.6 \mu\text{m}$ , and the thickness of a wall is 800 nm. In conventional TPP, the optimal resolution (the minimum distance between resolvable features) and minimum feature sizes (the smallest individual feature) are closely linked, as the

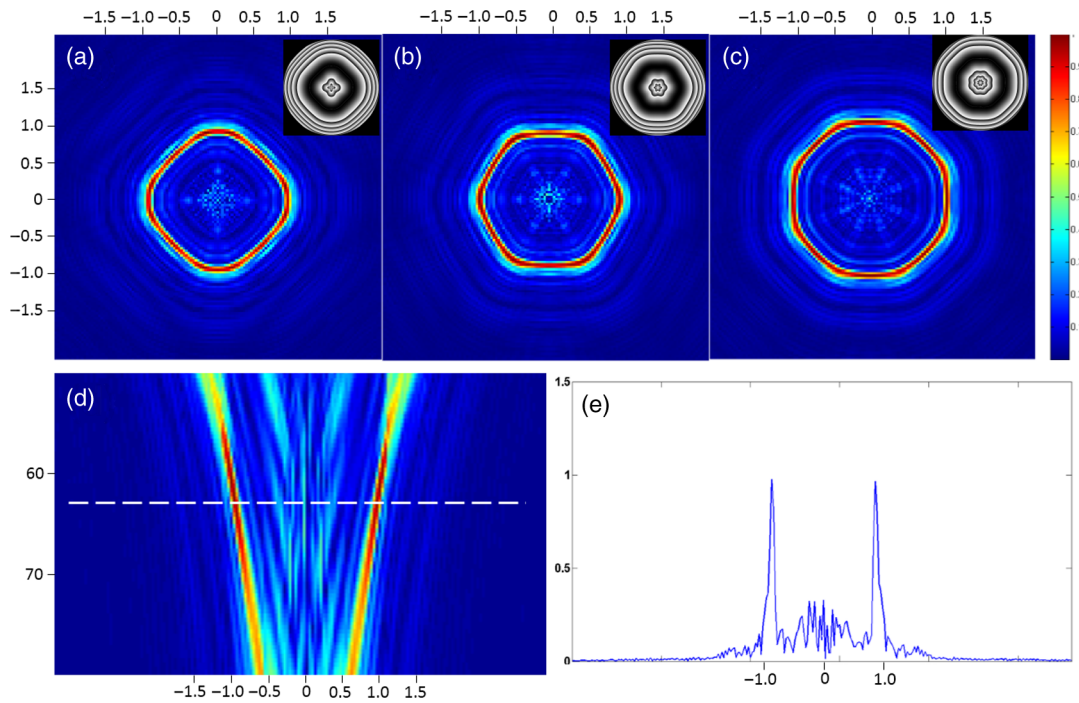


**Fig. 2** Simulation results of the illuminated field at the focal plane of (a) quadrangle, (b) hexagon, (c) octagon, and (d) Fresnel lens. (d) The intensity distribution at the meridian plane containing the optical axis of (a). The unit of coordinates in (a) to (d) is millimeters. (e) The cross-section intensity curve at the focal plane of (d). The x-axis shows the position of intensity; the unit is millimeters. The y-axis is the normalized power.

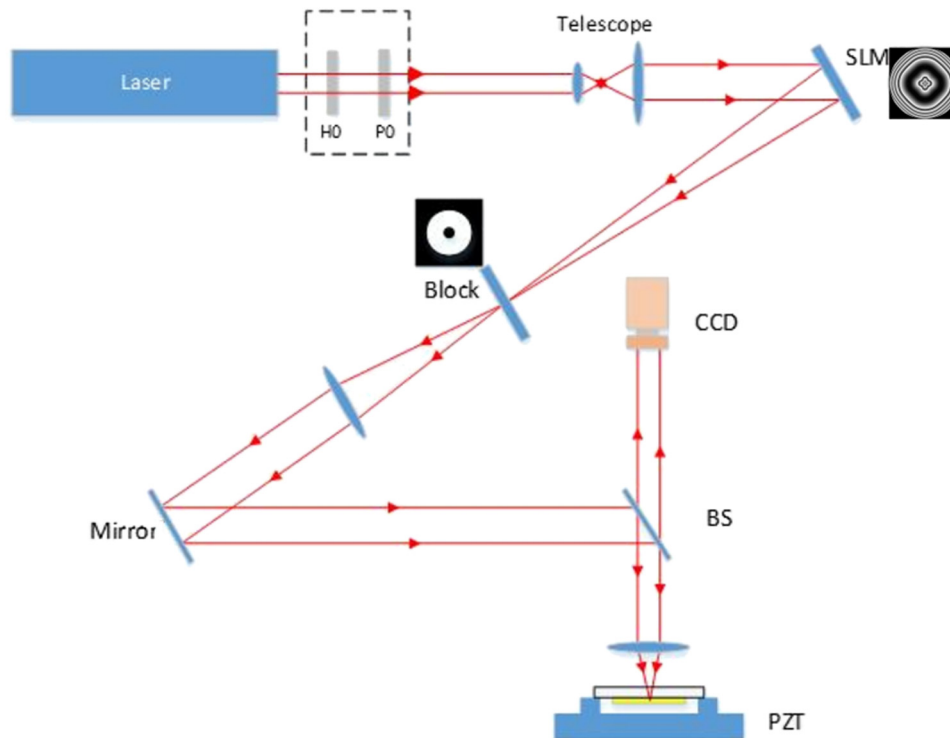


**Fig. 3** Diagram of the laser system. H0 is a half wave plate. P0 is a Glan laserprism. The PFL is loaded on the SLM. A high-pass filter is placed at the focus of the PFL to block the center beam.

fabrication process is point by point, and generally both can be  $\sim 100$  nm. However, in the focus-shaped approach that is presented here, large areas of photoresist are processed at once, and hence the optimal resolution is  $\sim \lambda$  (due to the

diffraction limit).<sup>25</sup> The height of the quadrangle corresponds to the thickness of the photoresist. By mixing with acetone at the volume ratio 1:5, and drop casting onto a cover glass, the thickness of spin-coated photoresist is  $8.5 \mu\text{m}$ . Figure 4(c) is

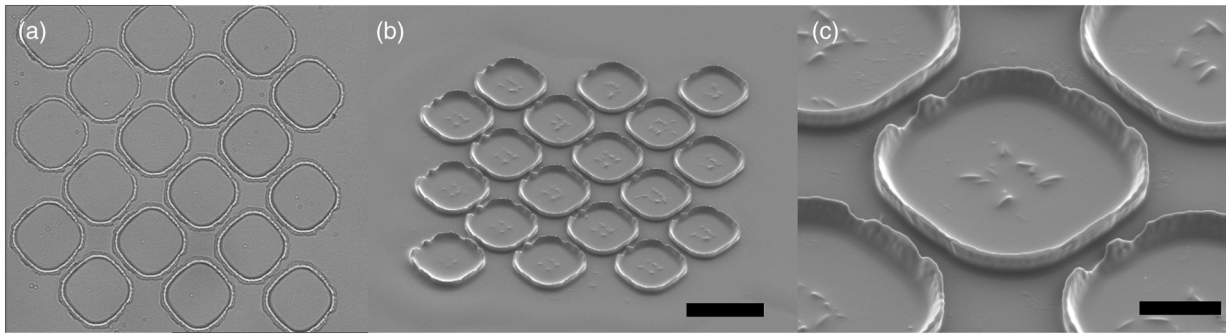


**Fig. 4** (a) The microscopy image, (b) SEM image, and (c) detail SEM image of quadrangle array fabricated by PFL. Scale bars are 40  $\mu\text{m}$  in (b) and 10  $\mu\text{m}$  in (c).

an SEM image of a quadrangle structure showing the detail 3-D profile of the fabricated quadrangle. Undesired structures appear at the center of quadrangle, which is mainly caused by the residual zero-order beam. It can be eliminated by a better high-pass filter. The wall of the quadrangle is slanted, making the structure bowl-like. It is similar to the simulation of the intensity distribution along Z-axis, as shown in Fig. 2(d).

Figure 5 is the SEM image of hexagon arrays. Two kinds of arrangement, the close-packed array and nonclose-packed array, are presented here. Each structure was fabricated by a single exposure for 400 ms, which is the same as that used in achieving quadrangle array. The photoresist was prepared with the same parameters as in Fig. 4, making the thickness of the sample 8.5  $\mu\text{m}$ . Figures 5(a) and 5(c) show the nonclose-packed hexagon array. The arrays have high uniformity in the morphology of each structure. The hexagons have rounded corners, which are designed to avoid an intensity peak at the apex of each corner of hexagons. Figures 5(b) and 5(d) are the close-packed hexagon arrays which look like honeycombs. The intensity peak at the corner makes the uniformity of wall thickness not as good as that in Figs. 5(a) and 5(c). But the whole morphology is sufficient for the potential use in cell feeding,<sup>26</sup> toxin absorption,<sup>27</sup> and so on. Compared with the nonclose-packed array, the honeycomb-shaped array can provide a 100% fill factor and more superficial area with smaller size.

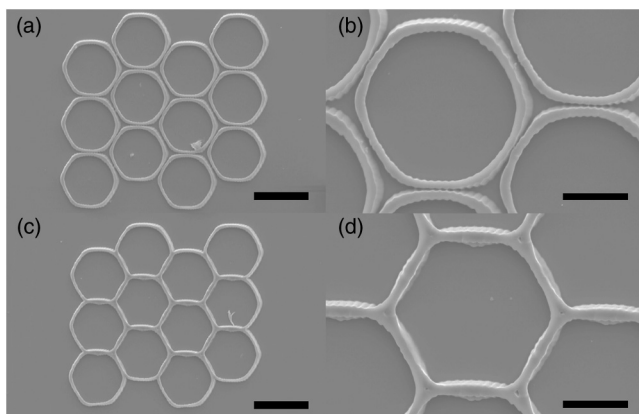


**Fig. 5** The SEM images of the nonclose-packed hexagon array [(a) and (c)] and closed-packed hexagon array [(b) and (d)]. Scale bars are 50  $\mu\text{m}$  in (a) and (c), 20  $\mu\text{m}$  in (b) and (d).

## 5 Conclusion

We have designed a PFL to generate a polygon-shaped light field in the focal plane. Using this Fresnel lens, a single exposure technique for the fabrication of a polygonal structure array via TPP was demonstrated. A close-packed hexagon array and nonclose-packed hexagon array were made to show the ability of this approach in fabricating honeycomb structures. This technique is much faster and more flexible than the conventional parallel fabrication using an array of beam spots. We anticipate this method will be used in fabrication of medical microdevices that can be applied in the fields of cell feeding, toxin absorption, and so on.

## Acknowledgments

National Natural Science Foundation of China (Nos. 51275502, 61475149, 51405464, 91223203, and 11204250); Anhui Provincial Natural Science Foundation (No. 1408085ME104); National Basic Research Program of China (No. 2011CB302100); the Fundamental Research Funds for the Central Universities (WK2090090012).

## References

1. D. Wu et al., "High efficiency multilevel phase-type fractal zone plates," *Opt. Lett.* **33**(24), 2913–2915 (2008).
2. C. Zhang et al., "An improved multi-exposure approach for high quality holographic femtosecond laser patterning," *Appl. Phys. Lett.* **105**(22), 221104 (2014).
3. Y. Hu et al., "High-efficiency fabrication of aspheric microlens arrays by holographic femtosecond laser-induced photopolymerization," *Appl. Phys. Lett.* **103**(14), 141112 (2013).
4. H. Xia et al., "Ferrofluids for fabrication of remotely controllable micro-nanomachines by two-photon polymerization," *Adv. Mater.* **22**(29), 3204–3207 (2010).
5. D. Wu et al., "Femtosecond laser rapid prototyping of nanoshells and suspending components towards microfluidic devices," *Lab Chip* **9**(16), 2391–2394 (2009).
6. Y. Hu et al., "Laser printing hierarchical structures with the aid of controlled capillary-driven self-assembly," *Proc. Natl. Acad. Sci. U. S. A.* **112**(22), 6876–6881 (2015).
7. Y. Hu et al., "Femtosecond laser induced surface deformation in multi-dimensional data storage," *Appl. Phys. Lett.* **101**(25), 251116 (2012).
8. J. Fischer et al., "The materials challenge in diffraction-unlimited direct-laser-writing optical lithography," *Adv. Mater.* **22**(32), 3578–3582 (2010).
9. S. Matsuo et al., "Femtosecond laser microfabrication of periodic structures using a microlens array," *Appl. Phys. A* **80**(4), 683–685 (2005).
10. Y. Hayasaki, "Holographic femtosecond laser processing and three-dimensional recording in biological tissues," *Prog. Electromagn. Res. Lett.* **2**, 115–123 (2008).
11. S. Hasegawa et al., "Holographic femtosecond laser processing with multiplexed phase Fresnel lenses," *Opt. Lett.* **31**(11), 1705–1707 (2006).
12. H. Takahashi et al., "Sparse-exposure technique in holographic two-photon polymerization," *Opt. Express* **16**(21), 16592–16599 (2008).

13. Y. Hu et al., "High-efficiency fabrication of aspheric microlens arrays by holographic femtosecond laser-induced photopolymerization," *Appl. Phys. Lett.* **103**(14), 141112 (2013).
14. Y. Tian et al., "High performance magnetically controllable microturbines," *Lab Chip* **10**(21), 2902–2905 (2010).
15. S. D. Gittard et al., "Fabrication of microscale medical devices by two-photon polymerization with multiple foci via a spatial light modulator," *Biomed. Opt. Express* **2**(11), 3167–3178 (2011).
16. S. J. Zhang et al., "Two-photon polymerization of a three dimensional structure using beams with orbital angular momentum," *Appl. Phys. Lett.* **105**(6), 061101 (2014).
17. L. Yang et al., "Two-photon polymerization of cylinder microstructures by femtosecond Bessel beams," *Appl. Phys. Lett.* **105**(4), 041110 (2014).
18. C. Zhang et al., "A rapid two-photon fabrication of tube array using an annular Fresnel lens," *Opt. Express* **22**(4), 3983–3990 (2014).
19. E. J. Smith et al., "Lab-in-a-tube: detection of individual mouse cells for analysis in flexible split-wall microtube resonator sensors," *Nano Lett.* **11**(10), 4037–4042 (2011).
20. G. Huang et al., "Rolled-up transparent microtubes as two-dimensionally confined culture scaffolds of individual yeast cells," *Lab Chip* **9**(2), 263–268 (2009).
21. K. Takei et al., "Out-of-plane microtube arrays for drug delivery—liquid flow properties and an application to the nerve block test," *Biomed. Microdevices* **11**(3), 539–545 (2009).
22. X. Yang, L. Wang, and S. Yang, "Facile route to fabricate large-scale silver microtubes," *Mater. Lett.* **61**(14), 2904–2907 (2007).
23. D. J. Thurmer et al., "Process integration of microtubes for fluidic applications," *Appl. Phys. Lett.* **89**(22), 223507 (2006).
24. J. W. Goodman, *Introduction to Fourier Optics*, pp. 52–53, Roberts and Company Publishers, Austin, Texas (2005).
25. B. Mills et al., "Single-pulse multiphoton polymerization of complex structures using a digital multimirror device," *Opt. Express* **21**(12), 14853–14858 (2013).
26. S. D. Gittard et al., "Fabrication of microscale medical devices by two-photon polymerization with multiple foci via a spatial light modulator," *Biomed. Opt. Express* **2**(11), 3167–3178 (2011).
27. F. Wang et al., "Hydrogel retaining toxin-absorbing nanosponges for local treatment of methicillin-resistant *Staphylococcus aureus* infection," *Adv. Mater.* **27**(22), 3437–3443 (2015).

**Chenchu Zhang** is a PhD candidate at the University of Science and Technology of China. He received his BS degree from Tianjin University in 2010. His current research interests include holographic beam shaping, rapid two-photon polymerization, and microfluidics.

**Yanlei Hu** is an associate professor at the University of Science and Technology of China. He received his doctorate and BS degrees at the University of Science and Technology of China in 2007 and 2012, respectively. His current research interests include femtosecond laser fabrication, digital holographic technology, micro/nanophotonics, and high density data storage.

**Dong Wu** is a professor at the University of Science and Technology of China. His research interests include micro optics, micro mechanics, and micro fluidics and bionics.

**Jiaru Chua** is a professor of University of Science and Technology of China. He received his doctorate and BS degree in University of Science and Technology of China in 1997 and 1985. His research topics include microelectronic mechanical systems and super precision measurement.

Biographies for the other authors are not available.